

# Electrochemistry in Self-Organized Dynamical States

## Current Oscillations and Potential Patterns in Electrocatalytic Reactions

by Peter Strasser

Self-organized spatiotemporal periodicities of chemical origin are prominent features of all living systems. Although to date no one has ever provided a clear reason as to why biochemical systems generally prefer operating in periodic or even more complex dynamical regimes, there is agreement that non-stationary regimes far from equilibrium could offer significant evolutionary advantages to regulatory chemical mechanisms when it comes to robustness and flexibility to external perturbations. Intrigued by the idea of unraveling the mechanisms of spatiotemporal dynamics in nature, researchers have been looking for simpler chemical model systems where certain dynamic aspects could be studied in more detail. One of the earliest model systems to be studied for its analogies to biology was the electrochemical passivation of metals. Ostwald,<sup>1</sup> Heathcote,<sup>2</sup> Lillie,<sup>3</sup> Bonhoeffer,<sup>4</sup> and Franck<sup>5</sup> extensively studied the propagation of passivation fronts on Fe wires to learn about the dynamics observed in transport of neural excitation. This presumably marked the first attempts to establish a relation between physiological and physicochemical rhythms.<sup>6</sup>

Spontaneous oscillations of current and potential, dating back as early as 1828,<sup>7</sup> have been observed in a large number of electrochemical systems, and there are probably more examples of electrochemical oscillatory systems to date than in any other branch of chemical kinetics. A review by Wojtowicz<sup>8</sup> summarized early research on temporal electrochemical oscillations. Early research on spatial pattern formation remained generally scarce with a few studies focusing on metal dissolution or metal passivation where the observation of patterns was straightforward.<sup>9,10</sup>

Yet, due to the seemingly tight grip of the second law of thermodynamics, periodic phenomena in chemistry were not accepted as reality or at best considered mere laboratory curiosities throughout the 19<sup>th</sup> and much of last century. Spontaneous oscillations around equilibrium, in fact, would require both the Gibbs free energy and

the entropy to oscillate, thereby violating the second law. Finally, the advent of non-equilibrium thermodynamics in the non-linear regime<sup>11</sup> and the concept of dissipative structures could resolve the dilemma. When maintained far from equilibrium and open to exchange of energy and/or matter with their surroundings, nonlinear chemical systems are able to self-organize taking on ordered states of locally decreased entropy such as temporally periodic, chaotic, or spatially periodic variations of concentrations of chemical species. Simultaneously, enhanced dissipation of energy through the system to the surroundings assures a net increase of entropy in accordance with the second law. Stopping the exchange of energy and matter, the system gradually approaches chemical equilibrium until all patterns cease. Electrochemical kinetics is inherently nonlinear, and electrochemical experiments are usually performed far from equilibrium. This may be one reason why so many self-organizing electrochemical systems have been found to date.

The past decade has witnessed renewed significant interest in the investigation of spatiotemporal electrochemical patterns.<sup>12-17</sup> Research groups focusing on nonlinear phenomena mushroomed, and three excellent review articles documented the drastic progress achieved in the understanding of temporal and spatial non-linear phenomena in electrochemistry.<sup>18-20</sup> Dealing with both similar empirical phenomena and models to describe, predict, and control dynamics, research on electrochemical patterns has moved close to such diverse disciplines as synergetics,<sup>21</sup> chaos theory,<sup>22</sup> and chronobiology,<sup>23</sup> and has thus evolved into a highly interdisciplinary field.

Aside from electrodisolution, numerous electrocatalytic systems became the focus of investigations. The observation of spatial inhomogeneities of concentration and potential across the electrified catalytic interface was challenging, because they are not visible as easily, compared to those in electrodisolution/passivation systems. One class of

self-organizing electrocatalytic systems was the electrooxidation of C1 fuels such as formic acid, which has been known for its oscillatory behavior almost 80 years.<sup>24</sup> Later on, the electrooxidations of formaldehyde and methanol<sup>25</sup> were also reported to exhibit oscillatory responses. These small organic compounds have recently attracted technological attention due to their potential applicability as liquid fuels in direct electrochemical energy conversion devices.<sup>26</sup> Knowledge of the full range of their kinetic behavior is therefore of interest for electrochemists and engineers alike.

This article addresses recent research on phenomena of spatiotemporal self-organization in electrochemical systems. It is written from the viewpoint of electrocatalysis as exemplified by the electrooxidation of formic acid. This overview is therefore by no means comprehensive and is unable to do justice to all types of oscillations and surface patterns observed in electrochemistry. It is primarily intended to create a sense of the surprising and (often visually) fascinating dynamic phenomena on electrified interfaces and to demonstrate the large scope for further work. The following sections also point out important mechanistic aspects of these experimental systems.

### Temporal Instabilities in Electrochemistry and Negative Impedance

Nonlinear chemical reaction systems, operated far from equilibrium, can exhibit a rich variety of dynamic states other than a single stationary state (monostability). In what is called a bifurcation, the non-equilibrium system switches from one type of dynamics to a qualitatively different one, as one or more control parameters (externally applied potential, bulk concentrations of educts, and temperature) are varied. In this respect, non-equilibrium bifurcations are very much like phase transitions in an equilibrium system. From concepts of nonlinear systems theory, dynamic states can be classified according to their complexity. The simplest instability involves two coexisting stable

steady states for a given set of control parameters (bistability). This transition between mono- and bistability is referred to as saddle-node bifurcation, and it gives rise to hysteresis behavior in current/potential curves. Spontaneous oscillations in physicochemical systems are generally related to the steady state becoming unstable in favor of a periodic orbit. The transition point is referred to as Hopf bifurcation. More complex bifurcations, finally, can lead to unstable periodic orbits and can result in complex chemical dynamics such as deterministic chaos.<sup>27</sup>

The origin of bistability and oscillations in electrochemical systems is schematically shown in Fig. 1. Electrochemical dynamics is generally described by the current balance between faradaic characteristics of interfacial processes, capacitive currents for charging the electrochemical double layer and the total migration current according to

$$I_{cap} + I_{far} = I_{mig} \quad (1)$$

or

$$C_{dl} \frac{\partial \phi}{\partial t} = -I_{far}(\phi) + I_{mig}(\phi) \quad (2)$$

where  $\phi$  and  $C_{dl}$  are the space and time-dependent interfacial potential (double-layer potential) and the interfacial capacity, respectively. Steady states are generally governed by the stationary current balance between  $I_{far}(\phi)$  and the current-voltage relation of the external circuit (load line) obtained by setting the left-hand side of Eq. 2 to zero. Assuming a linear potential drop inside the electrolyte under potentiostatic control, the load relation is given by  $I = I_{mig} = U/R - \phi/R$  where  $U$  is the applied constant potential and  $R$  denotes the uncompensated ohmic resistance. As long as the polarization curve  $I_{far}(\phi)$  is a monotonic function of the double layer potential (see Fig. 1a), there is only one steady state for all values of  $U$  and  $R$ . In contrast, if  $I_{far}$  exhibits a potential region of negative slope (Fig. 1b and 1c), there are values of  $U$  and  $R$  for which the dynamics exhibits two stable states on branches of positive slope and one unstable state on the middle branch (bistability, see Fig. 1c). Because the slope of the polarization curve is related to the sign of the electrochemical impedance, it follows that a negative impedance characteristic (negative differential resistance, NDR) in combination with a sufficiently large ohmic resistance  $R$  are necessary for temporal bistability.<sup>13, 19</sup> For spontaneous potentiostatic oscillations of  $I$  and  $\phi$  to occur

(constant applied potential  $U$ ), an additional essential dynamic variable has to be considered aside from the double layer potential  $\phi$ .

In the simplest case, the volume concentration  $c$  of a reactive chemical species near the interface can be taken into account resulting in an additional mass balance relation for  $c$ . Unlike the electrical variables,  $c$  is generally a slowly changing variable governed by the mass transfer from the bulk and the faradaic process consuming  $c$ . Figure 1d sketches out the phase space representation of a periodic orbit: The N-shaped curve and the straight line denote the stationary  $c - \phi$  values of the charge balance and mass balance, respectively. Again, the steady state marked by the intersection on the branch of negative impedance is unstable driving the system to relax on the N-shaped manifold. If the system is on the active branch of low values of  $\phi$  (high faradaic currents), the faradaic processes gradually consume  $c$ , and the operation point moves along the N-shaped curve toward smaller  $c$ . As the system reaches the extremum of the N-shaped curve, the system cannot help but relax to the passive branch (low faradaic current). As  $\phi$  is a very fast variable, this relaxation occurs very rapidly. The small current implies low rates of faradaic processes allowing  $c$  to replenish by diffusion. This, in turn, moves the system up along the N-shaped curve in Fig. 1c until the system relaxes back to its initial state concluding a periodic cycle. One can show that it is (1) the negative impedance; (2) a sufficiently large ohmic resistance; and (3) a

properly balanced difference in time scales between electrical and chemical variables that is crucial for the occurrence of spontaneous potentiostatic oscillations of the type outlined. The chemical origin of a negative impedance can be manifold. Typical examples in electrocatalytic reaction systems involve Frumkin-type double layer effects or the fast electroadsorption of catalytic active or poisoning surface species. In these electrochemical oscillators, the negative impedance is visible by an N-shaped  $I - U$  polarization curve with the Hopf bifurcation located on the middle branch of negative slope. Due to their simple mechanistic requirements, the outlined potentiostatic oscillations have been observed in a large number of experimental systems such as oxidation of cations, reduction of anions, and electrocrystallization.<sup>18,19</sup>

In the context of electrooxidations of small organic molecules, another mechanistic class of NDR-related electrochemical oscillators is of primary interest. Because its formal kinetic representation allows for a number of different chemical realizations, the current type of oscillator is to be characterized in the form that best matches the electrocatalytic system under discussion. First, a dominant faradaic process (current providing reaction) is involved that contributes the major portion of the total faradaic charge transfer. Being electrocatalytic, the current providing reaction typically requires a number of free active surface sites to occur. In the presence of a fast electroadsorbing surface species reducing the number of free surface sites, say, for

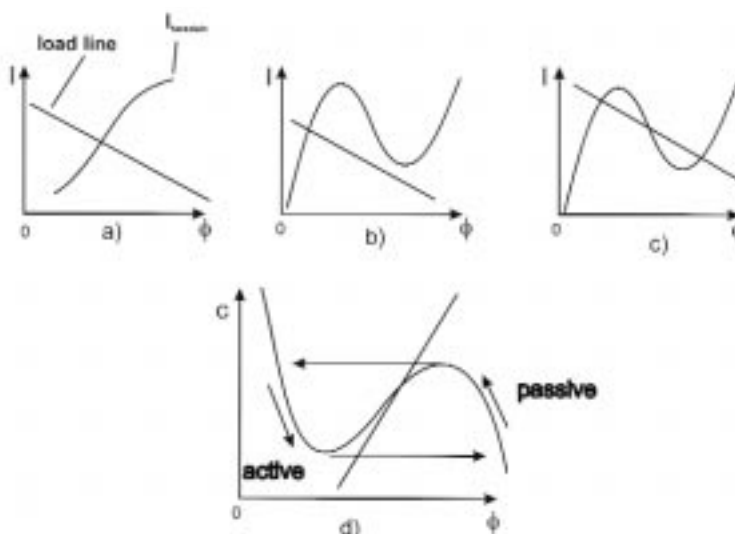


FIG. 1. Schematic illustration of the origin of electrochemical instabilities: (a) single stationary state (monostability) with load line  $I = U/R - \phi/R$  and monotonous faradaic  $I - \phi$  profile; (b) single stationary state with N-shaped faradaic characteristic; (c) three stationary states (bistability) at suitable values of  $U$  and  $R$ ; and (d) relaxation oscillations in an electrochemical two-variable system. The arrows indicate the trajectory of the periodic orbit within the  $c - \phi$  phase space.

large  $\phi$ , the resulting  $I_{far}(\phi)$  characteristic will exhibit a potential region of negative impedance on an anodic potential scan. Finally, if an additional electroadsorbing surface species adds to the mechanism, which is not consumed by the dominant faradaic process, and which adsorbs at small  $\phi$ , but desorbs at large  $\phi$ , then the overall system is able to exhibit both potentiostatic and galvanostatic oscillations for suitable values of the kinetic parameters. Although the chemical requirements necessary for oscillations seem demanding here, a surprisingly large number of oscillators of this type are known, most prominently the electrooxidations of small organic molecules such as formic acid.

In contrast to the oscillators outlined previously, the Hopf bifurcation is located on a  $I - U$  branch with positive slope, that is, the NDR crucial for the instability is not visible on the slow time-scale of the polarization curve. Hence, the NDR is hidden, and according to this distinctive feature, the oscillators are referred to as hidden-negative differential resistance oscillators (HNDR).<sup>19,20</sup> Impedance spectroscopy is a common tool to investigate the kinetics of electrochemical processes over a large range of frequencies. This makes it an ideal predictive technique to probe electrochemical systems for their capability to exhibit dynamical instabilities. Figure 2 shows the impedance diagram of the electroox-

idation of formic acid. Whereas the zero-frequency impedance is positive, a hidden NDR is obvious by the intersection of the impedance curve with the negative real axis at frequency  $\omega_0$  and impedance  $Z_0$ . Impedance spectra of this qualitative shape are characteristic of HNDR oscillators. The spectra are detectable at potentials where a Hopf bifurcation will occur if the ohmic resistance is sufficiently large. The quantitative predictive power of the impedance spectrum is reflected by the fact that  $\omega_0$  corresponds to the oscillation frequency at the Hopf bifurcation, while the ohmic resistance needed for the instability to occur at the considered potential is exactly given by  $-Z_0$ . Usually, for smaller absolute values of the applied potential at which the impedance is measured, the ohmic resistance  $-Z_0$  for inducing oscillations increases until the system can be destabilized by an infinite ohmic resistance only. This is the potential of the galvanostatic Hopf bifurcation indicated by a vanishing admittance.<sup>19</sup>

Figure 3a shows experimental current oscillations in voltammetric scans for the electrooxidation of formic acid on a Pt single crystal.<sup>28</sup> The sharp current spikes are indicative of sustained periodic rate oscillations. Due to the finite scan rate, the precise potential of the Hopf bifurcation is not resolved, which makes the oscillations appear abruptly with large amplitudes. Stopping the applied potential at various points along the anodic and cathodic scan results in sustained oscillatory time series as given in Fig. 3b.

For an understanding of the oscillatory mechanism, recall briefly the basic chemical mechanism of formic acid oxidation on Pt.<sup>26</sup> It is generally agreed that on Pt electrodes the formic acid molecule is oxidized through a dual-path mechanism involving the dissociative adsorption of formic acid on available bare surface sites followed by the formation of a reactive intermediate (*direct path*) and, in parallel, of surface-bonded carbon monoxide (*indirect path*). While the reactive intermediate quickly reacts to  $\text{CO}_2$ , adsorbed CO results in self-poisoning of the reaction rapidly reducing the overall reaction rate at small values of  $\phi$ . At higher overpotentials, fast adsorption of oxygen-containing species like water or OH is known to remove adsorbed CO by forming  $\text{CO}_2$ , thereby restoring high electrocatalytic activity. Based on the mechanistic findings, a realistic five-variable kinetic model has been developed<sup>29,30</sup> to account for the oscillatory instabilities.

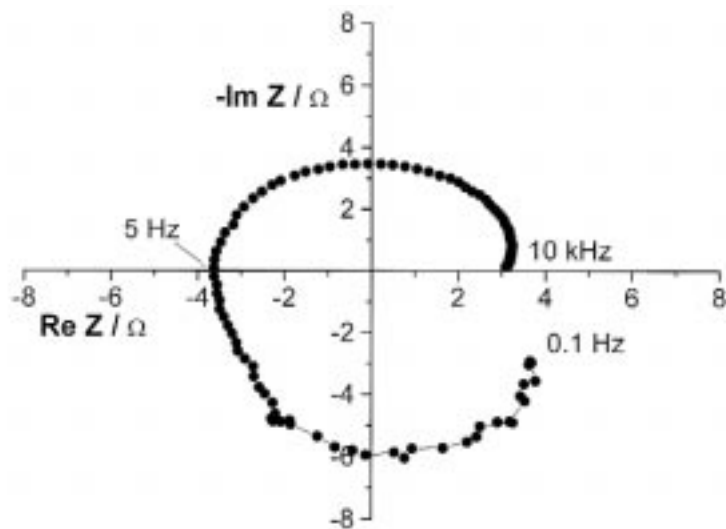


FIG. 2. Experimental impedance diagram for the electrooxidation of formic acid measured on sections of the polarization curve with positive slope. While positive at zero frequency, the impedance crosses the negative real axis at some finite frequency and resistance (hidden negative differential resistance) indicating a dynamic instability of the stationary state at that value of the uncompensated ohmic resistance. (0.1 M  $\text{HCOONa}/0.033 \text{ H}_2\text{SO}_4$ ,  $U=130 \text{ mV}$ ; reference electrode:  $\text{Hg}/\text{Hg}_2\text{SO}_4$ .)

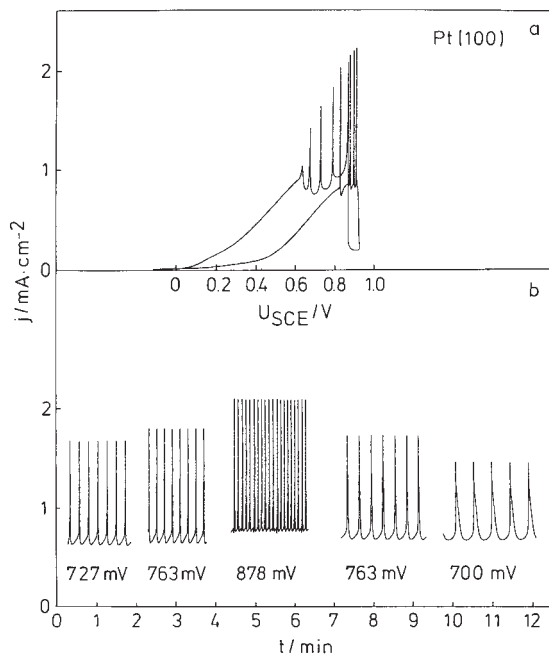


FIG. 3. (a) Cyclic voltammogram of electrooxidation of formic acid on a Pt(100) single crystal, current spikes indicating sustained current oscillations; and (b) current oscillations measured at various fixed potentials  $U$  (first three on anodic scan, last two on cathodic scan). (0.05 M  $\text{HCOOH}$ ,  $10^{-3} \text{ M HClO}_4$ , external ohmic resistance  $600 \Omega$ ,  $5 \text{ mV/s}$ .)

## Measurement of Electrochemical Patterns

There is experimental evidence that the oscillatory phenomena observed during the electrooxidations of C1-fuels such as formic acid, formaldehyde, and methanol can be traced back to a mechanism involving a hidden negative impedance similar to that outlined above. Therefore, they all fall into the mechanistic class of HNDR oscillators. Different oscillator classes generally require a distinctive set of mechanistic features regardless of their chemical realization. Mechanistic classification of unknown oscillatory systems can therefore provide valuable information for the analysis of complex reaction kinetics.<sup>28</sup>

### The Origin of Spatial Patterns in Electrochemistry

The previous section addressed temporal instabilities stemming from nonlinear electrochemical kinetics. Electrochemical spatial patterns involve the emergence of self-organized, inhomogeneous spatial distributions of the interfacial potential  $\phi$  along the electrode surface. Frequently, potential patterns are also accompanied by spatial variations of concentrations of surface species or volume species near the interface. Spatial inhomogeneities of  $\phi$  on electrodes obviously require some type of spatial communication or coupling across the electrode surface. Depending on their range, various types of coupling can be distinguished, namely short-range or local coupling, that is, when local perturbations only affect their immediate neighborhood, and global coupling, when local perturbations affect the entire spatial system with equal strength. In addition, the term non-local coupling has been coined for situations between the former two, that is, where the coupling between two points is long-range, but decreases in strength. Typical examples of local couplings in chemistry or surface catalysis involve heat and mass coupling by diffusion.<sup>31,32</sup>

The dominant coupling mechanism along electrochemical interfaces is electromigration, that is, the propagation of ions under the influence of a potential gradient. Generally, migration, just like diffusion, seeks to smooth out gradients and therefore exerts a positive coupling between surface locations. In contrast to diffusion, however, the effect of electromigration extends over a larger distance resulting in a positive nonlocal coupling.<sup>33</sup>

A very recent approach in tackling the electromigration expression in Eq. 2 was proposed by Christoph *et al.*<sup>34</sup> There, the migration current  $I_{mig}(\phi)$  was

recast in terms of an integral expression evaluated over the working electrode surface; the integral involved a coupling function  $H$  as a kernel, reflecting how strong two points across the electrode are coupled with each other. The function  $H$  turned out to be purely geometry dependent and needed to be computed only once during simulations of pattern formation. Figure 4 shows the shape of the coupling function for two distinct geometries.<sup>34</sup> The working electrode is assumed to be a thin ring with a point-like (Luggin-Haber) reference electrode located along the perpendicular axis of symmetry. The counterelectrode is assumed to be very distant from the ring. If the reference electrode is located far away (say several ring diameters), the nature of pure migration coupling becomes apparent, exhibiting a positive long-range coupling as given in curve A. If, however, the reference electrode is located in-plane with the ring electrode, a negative global offset is superimposed by the action of the potentiostat, giving rise to the overall coupling as shown by curve B. The surprising feature of the coupling in geometry B is that nearby points are coupled positively while remote points are coupled negatively; that is, a perturbation of the interfacial potential induces the opposite one on the other side of the ring. The impact of this unusual spatial coupling on the interfacial potential will be given below.

Electrochemical pattern formation involves self-organized macroscopic inhomogeneities of the potential at the electrolyte/electrode interface. If the change in potential involves visible modifications of the surface as in passivation, patterns can be observed directly.<sup>15</sup> In electrocatalysis, the interfacial potential distribution is usually not obvious. Therefore, all imaging methods, which are sensitive to changes in interfacial potential, yet non-invasive to the system, are suitable for measuring electrocatalytic patterns. Three methods have been used most widely. First, the earliest and simplest approach involves the use of potential microprobes to measure local interfacial potentials near the surface. The probe electrodes can either be arranged in an array along the surface of a static working electrode or; for instance, in a ring geometry, the electrode can be rotated near a single potential probe to obtain a continuous one-dimensional picture. Second, an array of small working electrodes can be employed to keep track of the space distribution of the migration currents. If one is interested in continuous patterns, however, it must be assured that the spacing of the individual electrodes does not alter the dynamics compared with a continuous electrode. Third, an elegant

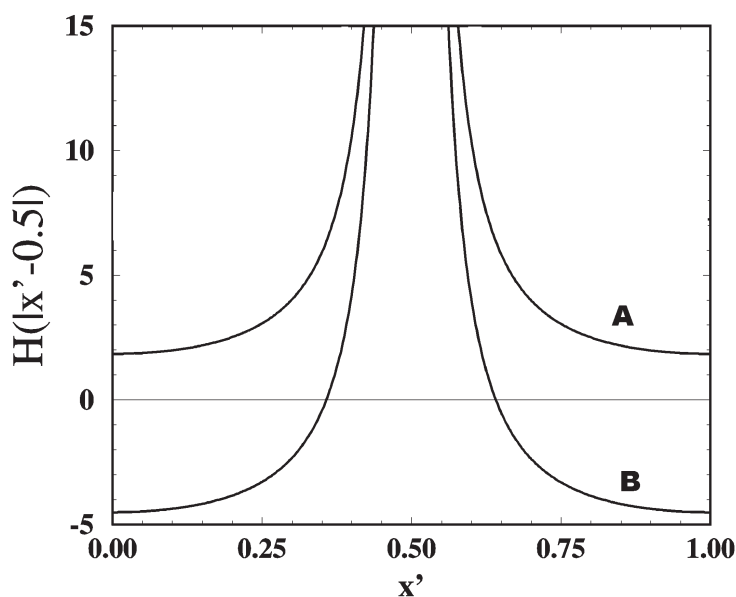


Fig. 4. Calculated electrochemical coupling function  $H$  for a thin ring electrode (periodic boundary conditions) with a point-like reference electrode placed along the central axis. (a) Reference electrode far from ring; and (b) reference electrode placed in-plane to ring electrode. The counter electrode is assumed to be at infinite distance, the length of the ring is normalized to 1. The function  $H(x', -0.5)$  illustratively represents the coupling strength between any two given points with distance  $x'$  along the ring. The functions shown arbitrarily assume one point to be at position 0.5.



way of monitoring one- and two-dimensional potential distributions at interfaces employs optical techniques like surface plasmon spectroscopy or electro-reflectivity measurements. Generally, these techniques exploit the dependence of the local optical parameters of metal surfaces on the local surface potential.<sup>35</sup>

Figure 5 depicts the experimental set-up with which the patterns discussed below were monitored.<sup>28</sup> A polycrystalline Pt ring electrode, a concentric counter electrode (not shown) and a Luggin-Haber reference electrode in the center of the ring formed a standard three-electrode set-up. The symmetric electrode geometry was deliberately chosen to allow for a comparison between experimental results and theoretical predictions. Eleven capillaries equipped with reference electrodes measured the local interfacial potential very near to the surface. At Position 12, a small insulated Pt wire served as trigger electrode to apply local perturbations in the interfacial potential. The

potentials of the potential probes were measured with respect to the working electrode and therefore represented a measure of the instantaneous local double layer potential.

### Patterns in Electrocatalysis

Prepared in a metastable passive state, a bistable system, which is locally activated by a supercritical perturbation, generally exhibits propagating passive-active fronts until the entire system has become active. This behavior is shown in Fig. 6a for the electrocatalytic oxidation of formic acid at potentials where a passive and active steady state coexist. The activation was applied at the location of the arrows (pulse electrode, Position 12) followed by the spreading of an active domain from Position 12 to Position 6. This behavior is in accordance with bistable catalytic reaction-diffusion systems such as the catalytic CO oxidation on Pt.<sup>31,32</sup>

Applying a local passivation to an already passive system, on the other

hand, does not result in front propagation in reaction-diffusion systems. A markedly different behavior can be observed in electrochemical reaction-migration systems as shown in Fig. 6b. The passivation at Position 12 induces an instantaneous activation at Position 6, leading to a spreading domain around Position 6 propagating toward where the perturbation was applied. This is analogous to the unusual observation of throwing a stone into a pond causing waves coming from the shore. The explanation lies in the shape of the coupling B in Fig. 4—local passivation translates into remote activation.<sup>17</sup> In addition, due to the space-dependent strength of the coupling, the activation remains fairly localized to form an active nucleus. Interestingly, Fig. 6 also reveals that the front velocity is non-monotonic, in fact, it is slowing down during most of the transition. This slowing down is also caused by the negative global offset of H.

Another manifestation of the long-range negative coupling becomes obvious if one measures the spatial distribution of the local interfacial potential near a Hopf bifurcation as shown in Fig. 7.<sup>36</sup> Rather than staying in a homogeneous regime, the system slips spontaneously into a symmetry-broken oscillatory state. While one half of the Pt electrode exhibits a high catalytic activity (low local potentials), the other half is CO poisoned with the local potentials being high. At two Positions (6 and 12), the amplitude is very much reduced by what corresponds to a kind of node of the anti-phase behavior. The overall pattern is reminiscent of an oscillatory standing wave. It can be shown that the negative coupling between opposite locations on the electrode induces the spatial instability of the homogeneous steady state at a more cathodic potential compared to that of the Hopf bifurcation.

The last example of a spontaneous pattern due to migration coupling under the influence of a negative global offset is shown in Fig. 8. Here, the applied potential is past the Hopf bifurcation. The standing waves have transformed into what can be considered as a travelling electrocatalytic pulse that continuously cycles around the working electrode, reactivating the poisoned surface periodically. Again, the coupling favors spatially inhomogeneous dynamic states rather than oscillations between all-active and all-passive operation points.

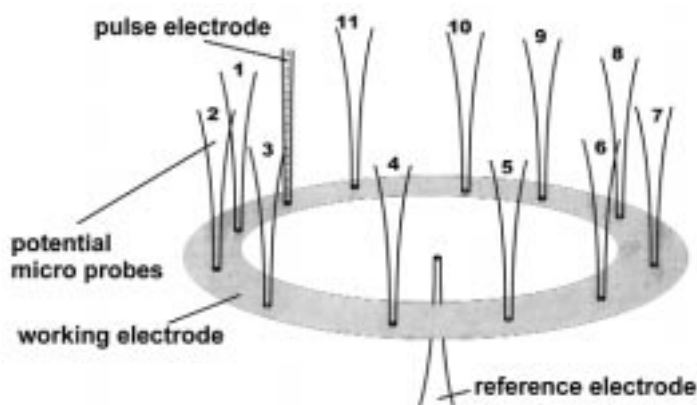


Fig. 5. Experimental set-up for the measurement of the distribution of the local potential near the surface of a ring electrode. Both potential probes and the reference electrode are Hg/Hg<sub>2</sub>SO<sub>4</sub> electrodes. The local potentials reported in the figures below were obtained with respect to the working electrode potential.

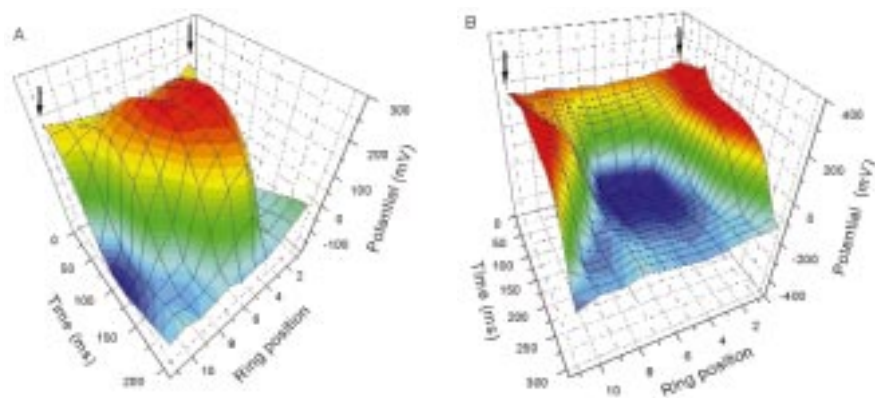


Fig. 6. (a) Local triggering of travelling electrocatalytic fronts. Prepared in a surface-poisoned, passive state (large local potential at  $t=0$ ), the bistable reactive system was locally activated at Position 12 (arrows). An active domain started to spread from where the perturbation was applied. (b) Remote triggering of travelling electrocatalytic fronts. After local passivation at Position 12, the passive system responded by an active domain emanating from the opposite Position 6.

## Outlook

This article has discussed self-organized spatiotemporal behavior in nonlinear electrochemical systems as exemplified by the electrocatalytic oxidation of small organic molecules such as formic acid. However, a number of important spatial-pattern forming mechanisms and their relation to electrochemistry have not been addressed, such as chaotic states,<sup>14</sup> Turing structures,<sup>37</sup> and patterns under galvanostatic conditions.<sup>12</sup>

The unusual spatial couplings generally found in electrochemistry will continue to spark basic research related to nonlinear systems theory in order to explore the dynamics of physico-chemical systems. In particular, surface patterns under more complex electrode geometries such as ribbons and disks will be likely the subject of future investigations. In a more biological context, recent progress in unraveling the nature of non-local migration couplings across electrified interfaces appears valuable for a better understanding of certain electrophysiological phenomena such as the transmission of neural excitation along neuron membranes.

On the engineering side, it has been suggested over a decade ago that certain nonlinear features of chemical systems, e.g., the continuous control over the phase shift between fluxes and forces through periodic perturbations, can be exploited for superior non-stationary operation points in terms of efficiency compared to stationary states.<sup>38,39</sup> This idea has recently attracted renewed interest in the context of electrochemical energy conversion devices.<sup>40</sup> Aside from temporal aspects, control of spatial couplings across electrified interfaces may provide interesting applications. For example, electrochemical devices are conceivable where local activation of a poisoned electrocatalytic surface is sufficient to restore complete activity, if the interface supports propagating active fronts. Further, as a negative global coupling never allows for a surface to become homogeneously poisoned, it may prove advantageous to operate self-poisoning processes under such dynamic conditions. ■

## Acknowledgments

I wish to express my thanks to J. Christoph for years of fruitful collaboration and his ingenious ways for adding meaning to complex experimental electrochemical dynamics. I am also grateful to J. Lee, M. Eiswirth, J.

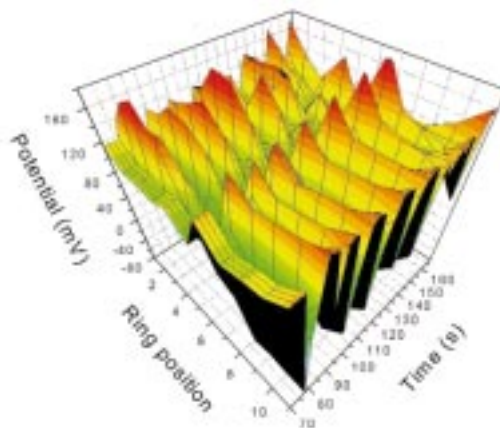


FIG. 7. Oscillatory standing wave patterns during electrooxidation of formic acid on Pt.

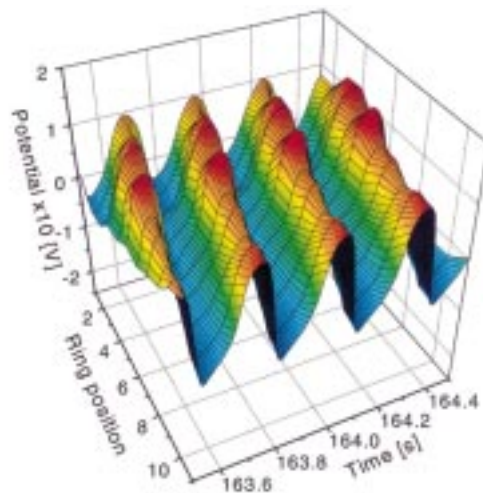


FIG. 8. The spatial potential profile during formic acid oxidation on an adatom-modified Pt ring electrode reveals an electrocatalytic pulse, propagating along the ring.

Hudson, and G. Ertl for many helpful discussions. This research was supported by grants and scholarships by the Deutsche Forschungsgemeinschaft and in part by the Studienstiftung des Deutschen Volkes.

## References

1. W. Ostwald, *Z. Phys. Chem.*, **35**, 204 (1900).
2. H. Heathcote, *J. Soc. Chem. Ind.*, **26**, 899 (1907).
3. R. Lillie, *Science*, **48**, 51 (1918).
4. K. Bonhoeffer, *Z. Elektrochem*, **47**, 147 (1941).
5. U. Franck, *Z. Elektrochem*, **55**, 154 (1951).
6. R. Lillie, *Science*, **67**, 593 (1928).
7. M. G. T. Fechner, *Schweigger J. für Chemie Physik*, **53**, 129 (1828).
8. J. Wojtowicz, in *Modern Aspects of Electrochemistry*, Vol. **8**, J. Bockris and B. Conway, Editors, p. 47, Butterworths, London (1973).
9. A. G. E. Smith, *Physiologist*, **4**, 112 (1961).
10. A. Pigeaud and H. Kirkpatrick, *Corrosion*, **25**, 209 (1969).
11. I. Prigogine, *Introduction to Thermodynamics of Irreversible Processes*, Wiley, New York (1961).
12. O. Lev, M. Sheintuch, L. Pismen, and C. Yarnitzky, *Nature*, **336**, 488 (1998).
13. M. T. M. Koper, *Electrochim. Acta*, **37**, 1771 (1992).
14. J. L. Hudson, in *Chaos in Chemistry and Biochemistry*, R. J. Field and L. Gyrgi, Editors, p. 123, World Scientific (1993).
15. R. Otterstedt, P. Plath, N. Jaeger, and J. Hudson, *Phys. Rev. E*, **54**, 3744 (1996).
16. G. Flätgen, K. Krischer, B. Pettinger, K. Doblhofer, H. Junkes, and G. Ertl, *Science*, **269**, 668 (1995).
17. J. Christoph, P. Strasser, M. Eiswirth, and G. Ertl, *Science*, **284**, 291 (1999).
18. J. L. Hudson and T. T. Tsotsis, *Chem. Eng. Sci.*, **49**, 1493 (1994).
19. M. T. M. Koper, *Adv. Chem. Phys.*, **92**, 161 (1996).
20. K. Krischer, in *Modern Aspects in Electrochemistry*, **32**, J. O. Bockris, B. Conway, and R. E. White, Editors, p. 1, Plenum Press, New York (1999).
21. H. Haken, *Synergetik 2. Aufl.*, Springer-Verlag, New York (1983).
22. M. Cross and P. Hohenberg, *Science*, **263**, 1569 (1994).
23. J. Murray, *Mathematical Biology*, Springer, Berlin (1990).

(continued on next page)

24. E. Mueller, *Z. Elektrochem.*, **28**, 101 (1992).
25. R. P. Buck and L. R. Griffith, *J. Electrochem. Soc.*, **109**, 1005, (1962).
26. R. Parsons and T. VanderNoot, *J. Electroanal. Chem.*, **257**, 9 (1988).
27. S. K. Scott, *Chemical Chaos*, Oxford University Press, Oxford (1991).
28. P. Strasser, PhD Thesis, Freie Universität Berlin, Berlin, Germany (1999).
29. P. Strasser, M. Lübke, F. Raspel, M. Eiswirth, and G. Ertl, *J. Chem. Phys.*, **107**, 979 (1997).
30. P. Strasser, M. Eiswirth, and G. Ertl, *J. Chem. Phys.*, **107**, 971 (1997).
31. G. Ertl, *Science*, **254**, 1750 (1991).
32. M. Eiswirth, M. Bär, and H. Rothermund, *Physica D*, **84**, 40 (1995).
33. G. Flätgen and K. Krischer, *Phys. Rev. E*, **51**, 3997 (1995).
34. (a) J. Christoph, R. Otterstedt, M. Eiswirth, N. Jaeger, and J. Hudson, *J. Chem. Phys.*, **110**, 8614 (1999); (b) J. Christoph, PhD Thesis, Freie Universität Berlin, Berlin, Germany (1999).
35. *Imaging of Surfaces and Interfaces: Frontiers of Electrochemistry*, J. Lipkowski and P. Ross, Editors, VCH (1999).
36. P. Strasser, J. Christoph, W.-F. Lin, M. Eiswirth, and J. Hudson, *J. Phys. Chem A*, **104**, 1854 (2000).
37. N. Mazouz and K. Krischer, *J. Phys. Chem. B*, **104**, 6081 (2000).
38. M. Schell, H. Schram, and J. Ross, *J. Chem. Phys.*, **88**, 2730 (1988).
39. M. Schell, F. N. Albahadilny, and J. Safar, *J. Electroanal. Chem.*, **353**, 303 (1993).
40. U. Stimming *et al.*, World IPO Pat. WO 98/42038 (1998); D. Wilkinson *et al.*, U.S. Pat. 6,096,448 (2000).

### About the Author

Trained as a physical chemist at Stanford University and Tuebingen University, Germany, **Peter Strasser** completed his PhD with Professor Ertl at the Fritz-Haber-Institut of the Max-Planck-Society, Berlin.

He is currently working as a project leader in the electronic materials division at Symyx Technologies, Santa Clara, California, on the development and application of combinatorial strategies for the discovery of materials for electrocatalysis and gas-phase catalysis by high-throughput methods. He can be reached via email at: [pstrasser@symyx.com](mailto:pstrasser@symyx.com).